

RESEARCH PAPER

White matter imaging helps dissociate tau from TDP-43 in frontotemporal lobar degeneration

Corey T McMillan,¹ David J Irwin,^{1,2} Brian B Avants,³ John Powers,¹ Philip A Cook,³ Jon B Toledo,² Elisabeth McCarty Wood,² Vivianna M Van Deerlin,² Virginia M-Y Lee,² John Q Trojanowski,² Murray Grossman¹

► Additional material is published online only. To view please visit the journal online (<http://dx.doi.org/10.1136/jnp-2012-304418>).

¹Department of Neurology, Perelman School of Medicine, Frontotemporal Degeneration Center, University of Pennsylvania, Philadelphia, Pennsylvania, USA

²Department of Pathology & Laboratory Medicine, Perelman School of Medicine, Center for Neurodegenerative Disease Research, University of Pennsylvania, Philadelphia, Pennsylvania, USA

³Department of Radiology, Penn Imaging and Computing Science Laboratory, University of Pennsylvania, Philadelphia, Pennsylvania, USA

Correspondence to

Dr Corey T McMillan, Department of Neurology, Perelman School of Medicine, Frontotemporal Degeneration Center, University of Pennsylvania, 3400 Spruce Street, 3 West Gates, Philadelphia, PA 19104, USA; mcmillac@mail.med.upenn.edu

Received 23 October 2012

Revised 21 January 2013

Accepted 5 February 2013

ABSTRACT

Background Frontotemporal lobar degeneration (FTLD) is most commonly associated with TAR-DNA binding protein (TDP-43) or tau pathology at autopsy, but there are no *in vivo* biomarkers reliably discriminating between sporadic cases. As disease-modifying treatments emerge, it is critical to accurately identify underlying pathology in living patients so that they can be entered into appropriate etiology-directed clinical trials. Patients with tau inclusions (FTLD-TAU) appear to have relatively greater white matter (WM) disease at autopsy than those patients with TDP-43 (FTLD-TDP). In this paper, we investigate the ability of white matter (WM) imaging to help discriminate between FTLD-TAU and FTLD-TDP during life using diffusion tensor imaging (DTI).

Methods Patients with autopsy-confirmed disease or a genetic mutation consistent with FTLD-TDP or FTLD-TAU underwent multimodal T1 volumetric MRI and diffusion weighted imaging scans. We quantified cortical thickness in GM and fractional anisotropy (FA) in WM. We performed Eigenanatomy, a statistically robust dimensionality reduction algorithm, and used leave-one-out cross-validation to predict underlying pathology. Neuropathological assessment of GM and WM disease burden was performed in the autopsy-cases to confirm our findings of an ante-mortem GM and WM dissociation in the neuroimaging cohort.

Results ROC curve analyses evaluated classification accuracy in individual patients and revealed 96% sensitivity and 100% specificity for WM analyses. FTLD-TAU had significantly more WM degeneration and inclusion severity at autopsy relative to FTLD-TDP.

Conclusions These neuroimaging and neuropathological investigations provide converging evidence for greater WM burden associated with FTLD-TAU, and emphasise the role of WM neuroimaging for *in vivo* discrimination between FTLD-TAU and FTLD-TDP.

INTRODUCTION

Frontotemporal lobar degeneration (FTLD) is the second most common presenile neurodegenerative disease¹ affecting approximately 20 per 100 000 adults under the age of 65.² From a pathological perspective, FTLD is a heterogeneous neurodegenerative disease with distinct underlying histopathological abnormalities. Approximately half of the FTLD patients have tau-positive inclusions (FTLD-TAU), whereas most of the remainder have an accumulation of TAR DNA-binding protein of ~43 kDa (TDP-43; FTLD-TDP).^{3,4} Some clinical-pathological evidence

suggests that syndromes of primary progressive aphasia (PPA) may be preferentially associated with one of these histopathological abnormalities,⁵ but syndromes such as behavioural-variant frontotemporal dementia (bvFTD) are equally likely to have FTLD-TAU and FTLD-TDP.⁶ As potential disease-modifying treatments emerge that target tau or TDP-43, it is critical to establish *in vivo* diagnostic methods that are sensitive and specific to these histopathological abnormalities.

Previous attempts to establish *in vivo* diagnostic methods for discriminating between underlying pathologies in FTLD have been largely observational. One study identified a series of clinical and behavioural features and used a clustering algorithm that suggested that poor planning was associated with FTLD-TAU, whereas poor personal conduct was associated with tau-negative FTLD.⁷ More recently, a proteomic cerebrospinal fluid (CSF) study suggested that a combination of five CSF analytes can achieve high sensitivity (86%) and modest specificity (78%) for differentially identifying FTLD-TDP relative to FTLD-TAU.⁸

In the present study, we take a hypothesis-driven approach based on previous neuropathological observations of these diseases to predict underlying pathology in individual patients. Specifically, FTLD-TAU, such as corticobasal degeneration, has characteristic tau inclusions throughout both grey matter (GM) and white matter (WM),⁹ whereas TDP-43 histopathological burden appears to be more prevalent in GM with relative sparing of WM.¹⁰ Therefore, an *in vivo* method of evaluating WM integrity, such as diffusion tensor imaging (DTI) of WM, may provide a sensitive and specific method that helps discriminate between FTLD subtypes.

Neuroimaging studies of WM in FTLD have been rare and suggest that FTLD-TAU and FTLD-TDP have reduced WM volume relative to older controls.^{11,12} One study reported that FTLD-TAU has reduced WM volume in the genu and anterior corpus callosum relative to FTLD-TDP.¹¹ However, volumetric analyses of WM, unlike DTI, do not accurately reflect microstructure changes in WM tracts. DTI studies suggest that fractional anisotropy (FA) is reduced in autopsy-confirmed FTLD compared with Alzheimer's disease (AD).^{13,14} However, we are unaware of an evaluation of DTI for establishing an *in vivo* diagnosis of underlying FTLD-TAU and FTLD-TDP histopathological abnormalities in individual cases.

To cite: McMillan CT, Irwin DJ, Avants BB, *et al.* *J Neurol Neurosurg Psychiatry* Published Online First: [please include Day Month Year] doi:10.1136/jnp-2012-304418

Neurodegeneration

Table 1 Mean (SE) demographic and clinical profiles of autopsy-confirmed and genetic surrogate patients with FTLD-TDP and FTLD-TAU

Group*	Group	N (Female)	Age	Education	Duration	MMSE
FTLD-TDP	Total	25 (13)	61.6 (1.4)	14.8 (0.7)	2.9 (0.5)	23.0 (1.3)
	Autopsy	6 (2)	58.5 (2.4)	16.7 (1.9)	2.7 (1.0)	23.0 (2.0)
	<i>C9ORF72</i>	12 (5)	61.3 (1.6)	14.9 (0.7)	3.5 (1.0)	25.8 (1.0)
	<i>GRN</i>	7 (6)	64.7 (3.3)	13.1 (1.6)	2.1 (0.3)	17.2 (3.5)†
FTLD-TAU	Total	10 (6)	62.2 (5.3)	15.4 (0.9)	2.8 (0.5)	20.7 (3.3)
	Autopsy	7 (4)	67.1 (6.2)	15.4 (0.9)	3.2 (0.6)	19.2 (4.3)†
	<i>MAPT</i>	3 (2)	50.7 (7.5)	15.3 (2.4)	1.7 (0.9)	23.7 (5.4)

*T tests confirmed that FTLD-TDP and FTLD-TAU were matched for age at MRI ($t(33)<1$; $p>0.1$), education ($t(33)<1$; $p>0.1$), disease duration ($t(33)<1$; $p>0.1$) and disease severity measure using the Mini Mental State Examination (MMSE) ($t(31)<1$; $p>0.1$). A χ^2 analysis demonstrated that groups were matched for gender ($\chi^2=0.18$; $p>0.1$).

†MMSE was not available for one patient from each group.

FTLD, frontotemporal lobar degeneration.

METHODS

Participants

Thirty-five patients diagnosed with a neurodegenerative disease, who had either a detailed neuropathological diagnosis at autopsy or a pathogenic genetic mutation consistent with FTLD-TAU (*MAPT*) or FTLD-TDP (*GRN*; *C9orf72*) pathology, were recruited from the Penn Frontotemporal Degeneration Center at the University of Pennsylvania. All patients underwent both volumetric T1 MRI and diffusion-weighted image (DWI) scans. The FTLD subgroups were matched for age, education, disease duration and disease severity (table 1). Our study cohort included a range of clinical phenotypes that are summarised in online supplementary table S1. Written informed consent was obtained from all participants using a protocol approved by the University of Pennsylvania Institutional Review Board.

Neuropathological diagnosis

Thirteen patients had a detailed neuropathological examination at autopsy consistent with FTLD-TAU or FTLD-TDP as reported previously.¹⁵ Neuropathological diagnoses were established according to consensus criteria⁴ by an expert neuropathologist (JQT) using immunohistochemistry with established monoclonal antibodies specific for pathogenic tau (mAb PHF-1)¹⁶ and TDP-43 (mAbs p409/410 or 171).^{17–18} Six cases had disease consistent with FTLD-TDP and were further classified into harmonised FTLD-TDP subtypes.¹⁹ Seven cases were diagnosed with a disease consistent with FTLD-TAU. There were no significant differences in brain weight, duration between neuroimaging acquisition and neuropathological exam, postmortem interval or plaque score²⁰ between FTLD-TAU and FTLD-TDP subgroups. Specific neuropathological diagnoses are summarised in online supplementary table S2.

Semi-quantitative ratings (0=absent, 1=mild, 2=moderate and 3=severe) were used to assess the angular gyrus and adjacent WM in the superior longitudinal fasciculus identified on the basis of imaging results (see Results: Classification of FTLD-TAU and FTLD-TDP using fractional anisotropy). Two trained examiners used a consensus procedure to evaluate four neuropathological features: (1) intensity of WM degeneration was graded using luxol fast blue; (2) WM inclusion burden was determined based on the density of tau-positive lesions in FTLD-TAU and TDP-43-positive lesions in FTLD-TDP; (3) neuronal loss was assessed using H&E-stained slides; and (4) GM inclusion burden was determined based on the density of tau-positive lesions in FTLD-TAU and TDP-43-positive lesions in FTLD-TDP. To additionally evaluate the specificity of the imaging results (see below), we evaluate WM and GM inclusion

burden in the temporal cortex and adjacent uncinate fasciculus. To statistically evaluate group-level differences in neuropathological measures, we performed Mann–Whitney U tests.

We additionally used genetic mutations as a surrogate for FTLD pathology (see online supplementary materials for details) as reported previously.^{21–22} This included four patients who had a *MAPT* pathogenic mutation, which is exclusively associated with FTLD-TAU. Likewise, individuals with either a *C9orf72* expansion greater than 30 repeats (N=12) or a *GRN* pathogenic mutation (N=9), which are exclusively associated with FTLD-TDP, were included. Two of the *GRN* cases additionally had autopsy confirmation of FTLD-TDP and one *MAPT* case had autopsy-confirmed FTLD-TAU.

Volumetric T1 MRI acquisition and preprocessing

All participants underwent a structural T1-weighted MPRAGE MRI acquired from a SIEMENS 3.0T Trio scanner with an 8-channel coil using the following parameters: repetition time=1620 ms; echo time=3 ms; slice thickness=1.0 mm; flip angle=15°; matrix=192×256 and in-plane resolution=1.0 mm isotropic. MRI volumes were preprocessed using PipeDream (<http://sourceforge.net/projects/neuropipedream/>) and Advanced Normalization Tools (ANTs)²³ as reported previously.¹⁴ Briefly, PipeDream diffeomorphically deforms each individual dataset into a standard local template space using a procedure that is symmetric to minimise bias towards the reference space for computing the mappings and topology preserving to capture the large deformation necessary to aggregate images in a common stereotactic space. These algorithms allow template-based priors to guide cortical segmentation and compute GM cortical thickness in the subject image space.²⁴ Cortical thickness images were normalised to template space and smoothed using a 4 mm full-width-half-maximum Gaussian kernel.

DTI acquisition and preprocessing

DWIs were acquired with either a 30-directional or a 12-directional acquisition sequence. The former included a single-shot, spin-echo, diffusion-weighted echo planar imaging sequence (FOV=245 mm; matrix size=128×128; N-slices=57; voxel size=2.2 mm isotropic; TR=6700 ms; TE=85 ms; and fat saturation). In total, 31 volumes were acquired per subject, 1 without diffusion weighting ($b=0$ s/mm²) and 30 with diffusion weighting ($b=1000$ s/mm²) along with 30 non-collinear directions. The 12-directional DTI sequence included a single-shot, spin-echo, diffusion-weighted echo planar imaging sequence (FOV=220 mm; matrix size=128×128; N-slices=40; slice thickness=3 mm; TR=6500 ms and TE=99 ms). In total, 13 volumes were acquired per subject, 1 without

diffusion weighting and 12 with diffusion weighting along with 12 non-collinear directions. An equal proportion of data from each DTI sequence was available per subject group (approximately 25% 12-directional; 75% 30-directional; $\chi^2=0.03$, $p=0.98$), and thus there is unlikely to be DTI sequence bias across groups. To be conservative, we minimised any potential DTI sequence bias by including a nuisance covariate for DTI sequence in all DTI analyses.

DWIs were preprocessed using ANTs²³ and Camino²⁵ within the associated framework of PipeDream (<http://sourceforge.net/projects/neuropipedream/>) analysis. Motion and distortion artefacts were removed by affine coregistration of each DWI to the unweighted image. Diffusion tensors were computed using a weighted linear least-squares algorithm implemented in Camino. Each participant's T1 image was warped to the template via the symmetric diffeomorphic procedure in ANTs described above. Distortion between participants' T1 and DT images was corrected by regularised intrasubject registration of the FA image to the T1 image. The DT image was then warped to template space by applying the intrasubject (FA to participant T1) and intersubject (participant T1 to template) warps.

Neuroimaging analysis

To analyse cortical thickness and FA, we employed Eigenanatomy (available within the scan algorithm in the ANTs toolkit).²⁶ Eigenanatomy involves identifying volumes of interests (VOIs) composed of correlated voxels that maximally account for the greatest variance in the entire dataset.^{14 26} By reducing the dimensionality of the data from over 1 M voxels to N-1 Eigenanatomy VOIs, we can perform high-powered statistics. Eigenanatomy is based on sparse singular value decomposition and identifies the VOI that accounts for the greatest variance first, the second most variance second and so on. To identify these VOIs, all normalised GM thickness volumes are first transformed into a number of subjects (N) by number of cortical voxels matrix, where voxels are selected to lie within a GM cortical mask. Sparse singular value decomposition is then used to identify the first N sparse eigenvectors from the data matrix. The ANTs implementation of Eigenanatomy employs a sparseness penalty on the eigenvectors such that (1) the entries of the eigenvector are both sparse (ie, have many zero entries) and non-negative and (2) the non-zero voxels are clustered and exceed a cluster extent threshold (>50 adjacent voxels). The sparseness and non-negativity allows the eigenvectors to be interpreted as weighted averages of the original data, resembling a distributed version of a traditional region of interest. We refer to each of these distributed regions as an Eigenanatomy VOI. We employ an identical procedure for our analysis of FA by using a WM atlas²⁷ explicit mask to constrain analyses to regions of probabilistically likely WM tracts.

Classification analysis

To evaluate the ability of neuroimaging to discriminate between FTLD-TDP and FTLD-TAU, we performed leave-one-out linear logistic regressions for each modality (MRI, DTI). To identify the optimal model for each neuroimaging modality, we performed N-1 training logistic regressions by iteratively increasing the number of eigenvectors included in the model (eg, FTLD.GROUP~EIG₁; FTLD.GROUP~EIG₁+EIG₂+...EIG_{N-1}), and for each model we generated a prediction for the left-out patient. We then performed a receiver-operating characteristic (ROC) curve analysis using predicted data and selected the model that achieved the highest area under the curve (AUC). This revealed that the GM model that included the first three Eigenanatomy VOIs and the FA model that included the first

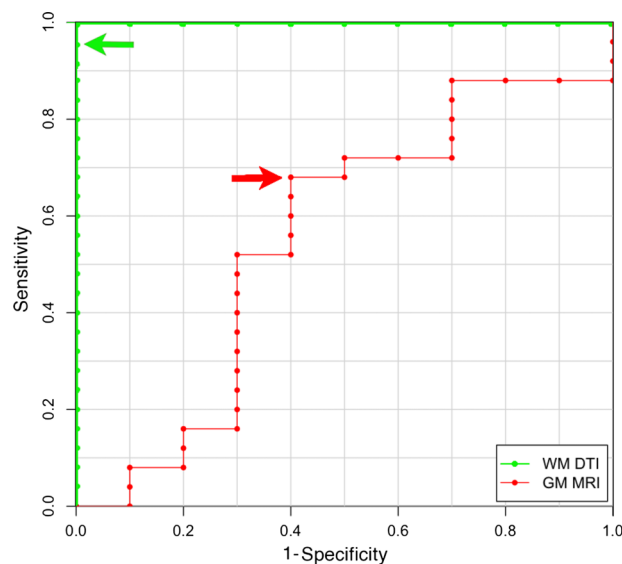


Figure 1 Receiver-operating characteristic curves illustrating sensitivity and specificity of diffusion tensor imaging classifiers of white matter (green) and cortical thickness classifiers of grey matter (red) for discriminating between frontotemporal lobar degeneration (FTLD)-TDP (sensitivity) and FTLD-TAU (specificity). Arrows indicate cut-off thresholds for each classifier.

Eigenanatomy VOI achieved the highest AUCs, respectively, 0.55 and 1.0. We report sensitivity and specificity for each selected model using an a priori defined probabilistic cut-off value of 0.714, because this proportion of patients was included in the FTLD-TDP group.

RESULTS

Classification of FTLD-TAU and FTLD-TDP using fractional anisotropy

An ROC curve analysis based on the logistic regression with the first FA eigenvector revealed 96% sensitivity and 100% specificity for classifying FTLD-TDP (figure 1). The FA eigenvector volume included two clusters located in the left and right superior longitudinal fasciculi (figure 2A). This FA eigenvector

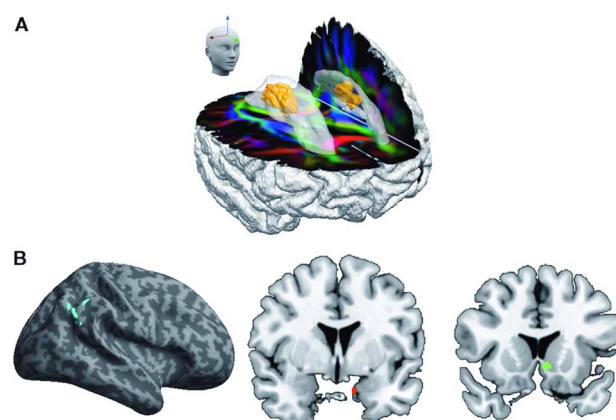


Figure 2 (A) Eigenanatomy volume of interest for fractional anisotropy with optimal classification of frontotemporal lobar degeneration (FTLD)-TDP and FTLD-TAU is highlighted in orange within the corpus callosum (opaque colour) overlaid on RGB image illustrating the direction of the white matter tracts (anterior-posterior=green; superior-inferior=blue; left-right=red); (B) Red, green and blue regions represent Eigenanatomy volumes of interest for grey matter cortical thickness with optimal classification of FTLD-TDP and FTLD-TAU.

Table 2 Neuropathological, genetic, clinical and demographic details for misclassified cases

Case	Neuropathological diagnosis/genetic mutation	Clinical phenotype	Demographic features*
White matter analysis misclassified case(s)			
WM.1	FTLD-TDP; intermediate tangles (Braak Stage III-IV)	bvFTD	MMSE=18
Grey matter analysis misclassified case(s)			
GM.1	Tauopathy NOS; <i>MAPT</i> (p.G389R)	bvFTD	MMSE=0
GM.2	<i>MAPT</i> pathogenic mutation (E10+16C>T)	PNFA	
GM.3	PSP	PSP	
GM.4	PSP	CBS	
GM.5	<i>C9orf72</i> expansion	PNFA	
GM.6	<i>C9orf72</i> expansion	bvFTD	Disease duration=8 years
GM.7	<i>C9orf72</i> expansion	bvFTD	Disease duration=7 years
GM.8	<i>C9orf72</i> expansion	bvFTD/ALS	
GM.9	<i>GRN</i> (p.V279GfsX5)	CBS	Education=6 years
GM.10	<i>GRN</i> (p.Thr272SerfsX10)	CBS	MMSE=12
GM.11	<i>GRN</i> (p.V90SfsX67)	CBS	
GM.12	FTLD with TDP-43 inclusions; <i>GRN</i> (p.R418X)	PNFA	
GM.13	FTLD with TDP-43 inclusions 114753	bvFTD	

Case numbers (eg, WM.1) provide an arbitrary label for each misclassified case.

*Only includes demographic features that differ more than 2.5 SD from means reported in table 1.

bvFTD, behavioural-variant frontotemporal dementia; FTLD, frontotemporal lobar degeneration; GM, grey matter; MMSE, Mini Mental State Examination; PSP, progressive supranuclear palsy; WM, white matter.

correctly classified all FTLD-TAU cases and 24 of 25 FTLD-TDP cases. Refer to table 2 for a description of the misclassified case.

Classification of FTLD-TAU and FTLD-TDP using grey matter thickness

An ROC curve analysis based on the logistic regression model included the first three GM Eigenanatomy volumes and revealed 64% sensitivity and 60% specificity for classifying FTLD-TDP (figure 1). The GM Eigenanatomy volumes, in order of accounted variance, included angular gyrus, amygdala and caudate (figure 2B). The misclassified cases included 4 out of 10 FTLD-TAU patients and 9 out of 25 FTLD-TDP patients (see table 2 for a summary of misclassified cases).

In order to evaluate whether there was a relationship between GM prediction and WM prediction, we additionally performed a correlation analysis (see online supplementary figure S1). This analysis revealed no significant relationship between GM and WM prediction accuracy ($r[33]=0.11$; $p>0.1$), suggesting that both modalities capture independent measures of pathology associated with FTLD.

Neuropathological evaluation in autopsy cohort

Mann-Whitney U comparisons evaluated pathological burden in the GM of the angular gyrus and the WM of the superior longitudinal fasciculus because these adjacent regions were implicated as having the greatest classification accuracy in both the GM and WM neuroimaging analyses. Representative samples of WM degeneration, WM inclusion burden, GM neuronal loss and GM inclusion burden for FTLD-TAU and FTLD-TDP are illustrated in figure 3. As summarised in figure 4, we observe a significant difference between FTLD-TAU and FTLD-TDP in measures of WM degeneration (Mann $U=5.5$; $p<0.05$) and WM inclusion burden (Mann $U=7.5$; $p<0.05$), with both measures being more severe in FTLD-TAU than FTLD-TDP. There was also a trend towards greater GM neuronal loss for FTLD-TDP relative to FTLD-TAU (Mann $U=10.0$; $p=0.09$). GM inclusions did not differ across pathological

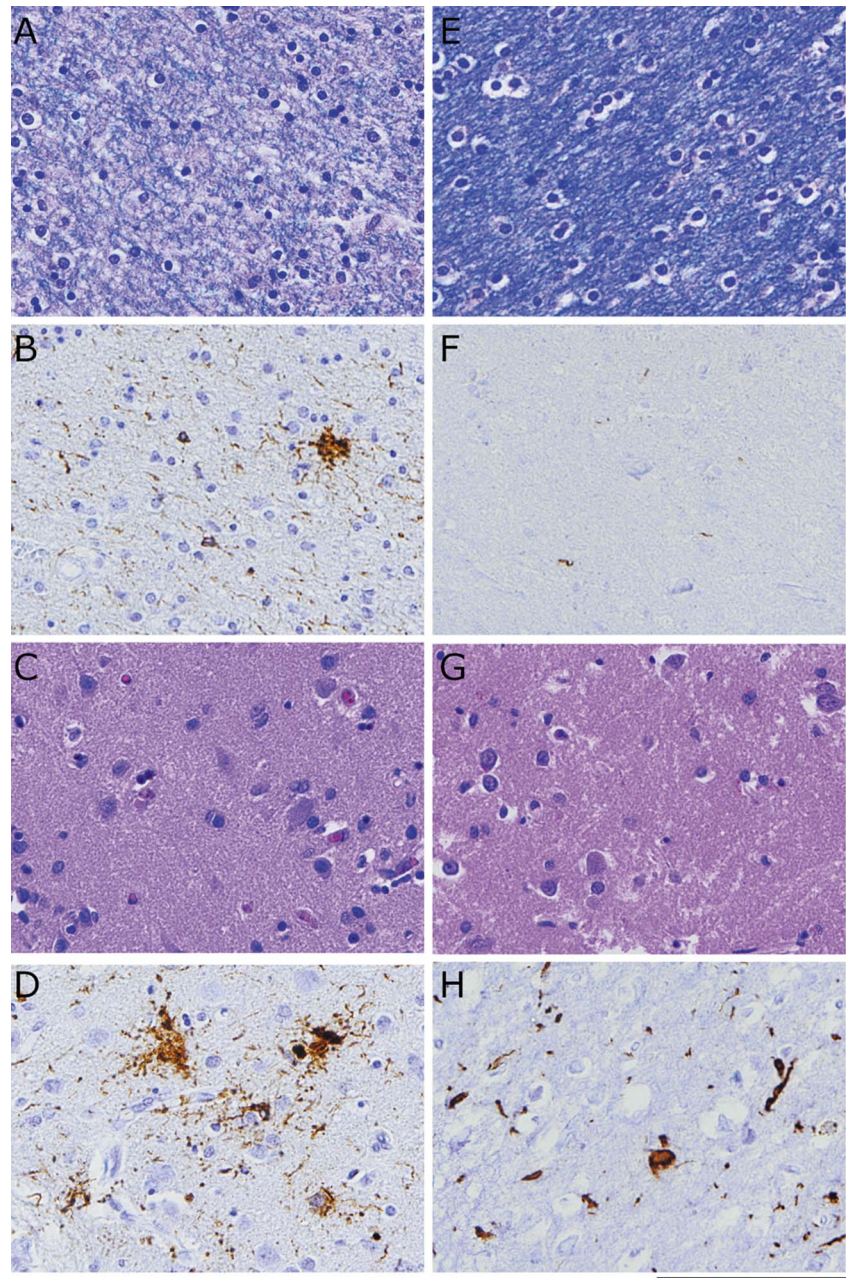
subtypes (Mann $U=19.0$; $p>0.10$). An evaluation of WM and GM inclusion burden in a control region in the temporal lobe and adjacent uncinate fasciculus, which was not implicated in the neuroimaging analyses, did not yield significant differences across groups: WM inclusion (Mann $U=28.5$; $p>0.10$) and GM inclusion (Mann $U=25.5$; $p>0.10$) burden. This suggests that the angular gyrus and adjacent superior longitudinal fasciculus are specific for discriminating between FTLD-TDP and FTLD-TAU. Together, these findings parallel our neuroimaging analyses and emphasise the contribution of WM analyses in the distinction between FTLD-TAU and FTLD-TDP.

DISCUSSION

FTLD is a heterogeneous neurodegenerative condition associated mainly with FTLD-TAU or FTLD-TDP pathology. Previous investigations have suggested significant GM and WM pathology in FTLD-TAU,⁹ whereas FTLD-TDP generally has greater GM than WM pathology.¹⁰ Our comparative neuroimaging analyses suggest that WM disease, as reflected in DTI measurements of FA, is significantly more prominent in FTLD-TAU than FTLD-TDP. These in vivo DTI measures of substantial WM disease in FTLD-TAU relative to FTLD-TDP were confirmed by ex vivo comparative neuropathological measures of WM in a subset of the same patients. GM measures showed differences between FTLD-TAU and FTLD-TDP as well, but were relatively modest. Thus, multimodal neuroimaging that includes DTI assessment of WM may be a promising biomarker that helps establish an in vivo diagnosis distinguishing between FTLD-TDP and FTLD-TAU in individual patients.

Previous group-level studies have shown that FTLD-TAU and FTLD-TDP have reduced WM volume relative to older controls,^{11 12} and one study reported that FTLD-TAU has reduced WM volume in the anterior corpus callosum relative to FTLD-TDP.¹¹ By comparison, previous group-level neuroimaging comparisons of GM in FTLD-TAU and FTLD-TDP using volumetric T1 MRI have yielded mixed results. Some work has found different patterns of GM atrophy in FTLD-TAU and FTLD-TDP,^{11 28} whereas others have reported no significant

Figure 3 Neuropathological evidence for a dissociation of grey matter (GM) and white matter (WM) burden in representative cases of frontotemporal lobar degeneration (FTLD)-TAU and FTLD-TDP at 40× (Scale bar represents 100 μm): (A) luxol fast blue (LFB) stain for WM degeneration for FTLD-TAU; (B) tau inclusions in WM for FTLD-TAU; (C) H&E stain for neuronal loss in GM for FTLD-TAU; (D) tau inclusions in GM for FTLD-TAU; (E) LFB stain for WM degeneration for FTLD-TDP; (F) TDP-43 inclusions in WM for FTLD-TDP; (G) H&E stain for neuronal loss in GM for FTLD-TDP; and (H) TDP-43 inclusions in GM for FTLD-TDP.



GM differences between FTLD-TAU and FTLD-TDP.¹² This is consistent with our observation that GM neuroimaging achieves only modest sensitivity and specificity for evaluating pathology in individual cases, and suggests that GM neuroimaging alone

may not be sufficient as a candidate biomarker for predicting histopathological abnormalities in FTLD.

Recent works suggest that multimodal imaging is helpful for in vivo diagnosis as the addition of WM neuroimaging to GM

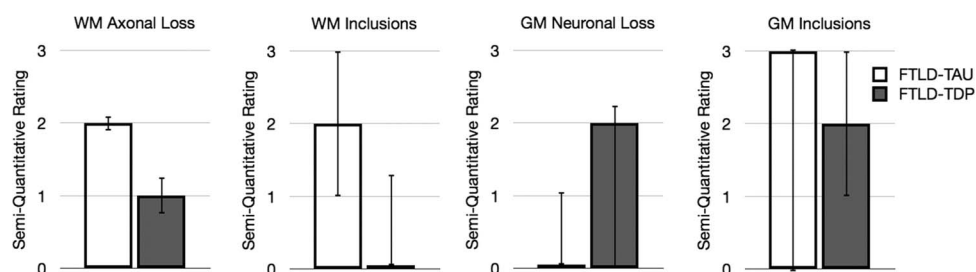


Figure 4 Median semi-quantitative ratings (IQR) for neuropathological measures of angular gyrus and adjacent white matter in the superior longitudinal fasciculus.

neuroimaging optimises discrimination between FTLT and AD.^{13 14} These previous findings may have been due in part to the WM changes in the subgroup of FTLT patients with tau pathology. In one previous study, GM and WM neuroimaging datasets were combined by using covariates for each modality in a logistic regression.¹³ In another study, the two modalities were combined statistically using a multivariate sparse canonical correlation analysis to evaluate how GM and WM changes associated with FTLT and AD were related to one another.¹⁴ In the current study, we did not evaluate a multimodal approach because WM alone achieved such high accuracy for discriminating between FTLT-TAU and FTLT-TDP, and there was a pathological basis for this observation. Additionally, our comparison of WM prediction to GM prediction suggested that both of these neuroimaging measures are independent from one another, which is consistent with our hypothesis that FA would capture WM pathology that is specific to FTLT-TAU.

Discrepancies between our findings and previous work failing to discriminate between FTLT-TAU and FTLT-TDP may have been due in part to our use of optimised imaging analysis procedures. Our use of Eigenanatomy benefits from massive data reduction therefore allows us to implement powerful prediction statistics.²⁶ In a previous study using a similar Eigenanatomy approach, we demonstrated that neuroimaging can be used to predict CSF analytes,²⁹ thereby reducing the need for repeated lumbar punctures during a treatment trial. Importantly, both the current study and previous work using Eigenanatomy rely on cross-validation and prediction-based statistics to illustrate a relationship between pathology and neuroimaging, and to demonstrate that neuroimaging can be used to derive specific predictions about pathology in individual patients.

We took advantage of previous neuropathological reports of significant WM disease burden in FTLT-TAU,⁹ but modest WM disease in FTLT-TDP, and used this observation to motivate an in vivo WM neuroimaging study to help distinguish between these histopathological subgroups. Our DTI results suggest that reduced FA in bilateral superior longitudinal fasciculus yields optimal classification accuracy for discriminating between FTLT-TAU and FTLT-TDP. A previous study from our lab also found reduced FA in superior longitudinal fasciculus in autopsy-confirmed patients with the non-fluent/agrammatic variant of PPA,³⁰ and sporadic forms of this clinical syndrome are more often associated with FTLT-TAU than FTLT-TDP pathology.⁵ This overlap between WM regions in the current study and a region observed in the clinicopathological study provides converging evidence that the superior longitudinal fasciculus is specific for FTLT-TAU. We confirmed our findings by observing significant WM degeneration and a higher rate of inclusions for FTLT-TAU compared with FTLT-TDP in this region and, importantly, WM and GM inclusion burden did not differ in a control region. It is unlikely that our findings are related to distinct subtypes of TDP-43 proteinopathy, which have varying degrees of neuronal loss and gliosis in WM.¹⁰ In our sample, most FTLT-TDP patients were TDP subtype A or B (5/6 88.3%), which contain a higher burden of TDP-43 immunoreactive glial pathology compared with, for example, subtype C.¹⁰ Another potential confound is that non-FTLT spectrum pathology can be intermixed in these diseases,³¹ but in our autopsy-confirmed sample, only one case of FTLT-TAU (progressive supranuclear palsy (PSP)) and one case of FTLT-TDP had sufficient density of neurofibrillary tangles and senile plaques to meet criteria for a secondary diagnosis of low-probability AD.³² Future validation studies that involve extensive training and testing procedures will be necessary to determine whether superior longitudinal

fasciculus is a 'signature region' of FTLT-TAU paralleling signature regions for AD.³³

This study provides the only report that we are aware of that evaluates in vivo neuroimaging and ex vivo neuropathological examination of specific histopathological abnormalities in the same neurodegenerative disease patient cohort. Despite the time delay between neuroimaging and autopsy, our observations suggest that the WM dissociation observed at autopsy between FTLT-TAU and FTLT-TDP is detectable at earlier stages of the disease using DTI. An important direction of future research will be to evaluate how different DTI measures (eg, radial diffusivity, axial diffusivity, mean diffusivity and FA) reflect fine-grained microstructural changes associated with specific histopathological abnormalities (eg, neuronal loss, axonal loss, demyelination). In the current study, we focused only on FA because at first evaluation this measure alone achieved high sensitivity and specificity.

An important caveat to consider when interpreting our findings is concerned with the clinical characteristics of our cohort. A shortcoming of pathological studies is that they are performed after end-stage disease when patients are typically too impaired to participate in a detailed clinical examination. Previous studies have investigated how the distribution of disease is modulated by underlying pathology in a single clinical phenotype and have achieved mixed findings. It has been reported that nonfluent/agrammatic primary progressive aphasia (naPPA) and logopenic variant primary progressive aphasia (lvPPA) have either a more anterior or a posterior distribution of GM disease depending on whether they have FTLT or AD pathology, respectively.³⁴ A study of the distribution of GM disease in an autopsy-confirmed behavioural-variant FTLT cohort revealed distinct patterns of atrophy depending on the source of FTLT pathology,²⁸ whereas a study of svPPA reported similar patterns of GM disease independent of different sources of FTLT pathology.³⁵ Importantly, none of these previous studies investigated how WM is affected by different sources of FTLT-TAU or FTLT-TDP pathology. There is some value in identifying diagnostic features that can discriminate between FTLT-TAU and FTLT-TDP, regardless of the clinical phenotype so that patients may be entered into a disease-modifying clinical trial with equal confidence. The current study combined samples with a range of clinical phenotypes, and, despite the clinical heterogeneity of our cohort, we observed that DTI may provide a promising biomarker for identifying whether living patients have FTLT-TAU and FTLT-TDP on an individual case-by-case basis.

Our study additionally contained some genetic heterogeneity, and we did not discriminate between different subtypes of FTLT-TAU or FTLT-TDP pathology. Previous studies have investigated GM neuroimaging in specific genetic mutations associated with FTLT and these may yield different distributions of disease compared with sporadic cases with the same underlying pathology.³⁶⁻³⁸ Also, finer-grained distinctions of FTLT subtype pathology relative to healthy cohorts have suggested that these may yield distinct patterns of atrophy.^{39 40} Additional work is needed to systematically evaluate neuroimaging in inherited and sporadic disorders with a range of clinical and pathological presentations to optimise the generalisability of neuroimaging biomarkers.

There are additional technical caveats to consider when interpreting our results. These are related to the relatively new emergence of high-quality DTI procedures in combination with a several-year duration between in vivo DTI acquisition and ex vivo neuropathological exam. First, given these limited samples, we were restricted to using leave-one-out cross-validation. As

more pathologically validated cases of high-resolution DTI data become available, we anticipate that we will be able to use more advanced classification algorithms, including the testing of our prediction algorithms in an independent dataset. Second, DTI data used in this prediction study was composed of a small proportion of lower resolution data (25%). It is possible that classification accuracy may be more accurate when using high-resolution datasets. Importantly, despite these technical limitations, we were able to reliably discriminate between FTLT-TAU and FTLT-TDP, and we were able to establish that our DTI results were convergent with WM measures of tissue pathology.

In conclusion, FTLT-TDP and FTLT-TAU appear to have distinct patterns of WM change in neuroimaging studies, paralleling our neuropathological observations. We found that DTI improves the ability to discriminate between histopathological subtypes of FTLT during life. In the context of a treatment trial, DTI may thus provide a promising, non-invasive screening measure that is both sensitive and specific. A multimodal neuroimaging approach that incorporates both T1 imaging of GM and DTI imaging of WM therefore may contribute to screening patients for treatment trials designed to target specific histopathological abnormalities.

Acknowledgements This work was supported in part by the Wyncote Foundation and the National Institutes of Health (T32-AG000255; NS065347; AG010124, AG032953, AG017586; AG000255; NS044266, AG015116, NS053488). JBT is supported by the Alfonso Martín Escudero Foundation. The authors would like to thank Dr Peter Davies for the kind gift of the paired-helical filament-1 monoclonal antibody used in our study.

Contributors The following authors contributed to this manuscript in the following ways: CTM, DJI, BBA and MG were involved in literature search; figures: CTM, DJI, JP and PC; CTM, DJI, BBA and MG were involved in study design; JP, EMW, VMVD, VM-YL, JQT and MG collected data; CTM, DJI, BBA, JBT, JP, PC, EMW, VMVD, VM-YL, JQT and MG were involved in data analysis; CTM, DJI, BBA, JBT, VM-YL, JQT and MG were responsible for data interpretation; and CTM, DJI, BBA, JBT, JP, PC, EMW, VMVD, VM-YL, JQT and MG were responsible for writing the manuscript.

Funding Wyncote Foundation, NIH, Alfonso Martín Escudero Foundation.

Competing interests None.

Ethics approval University of Pennsylvania Institutional Review Board.

Provenance and peer review Not commissioned; externally peer reviewed.

REFERENCES

- Ratnavalli E, Brayne C, Dawson K, *et al*. The prevalence of frontotemporal dementia. *Neurology* 2002;58:1615–21.
- Knopman DS, Roberts RO. Estimating the number of persons with frontotemporal lobar degeneration in the US population. *J Mol Neurosci* 2011;45:330–5.
- Mackenzie IRA, Neumann M, Bigio EH, *et al*. Nomenclature for neuropathologic subtypes of frontotemporal lobar degeneration: consensus recommendations. *Acta Neuropathol* 2009;117:15–18.
- Mackenzie IRA, Neumann M, Bigio EH, *et al*. Nomenclature and nosology for neuropathologic subtypes of frontotemporal lobar degeneration: an update. *Acta Neuropathol* 2010;119:1–4.
- Grossman M. Primary progressive aphasia: clinicopathological correlations. *Nat Rev Neurol* 2010;6:88–97.
- Josephs KA, Hodges JR, Snowden JS, *et al*. Neuropathological background of phenotypical variability in frontotemporal dementia. *Acta Neuropathol* 2011;122:137–53.
- Hu WT, Mandrekar JN, Parisi JE, *et al*. Clinical features of pathologic subtypes of behavioral-variant frontotemporal dementia. *Arch Neurol* 2007;64:1611–16.
- Hu WT, Chen-Plotkin A, Grossman M, *et al*. Novel CSF biomarkers for frontotemporal lobar degenerations. *Neurology* 2010;75:2079–86.
- Forman MS, Zhukareva V, Bergeron C, *et al*. Signature tau neuropathology in gray and white matter of corticobasal degeneration. *Am J Pathol* 2002;160:2045–53.
- Geser F, Martinez-Lage M, Robinson J, *et al*. Clinical and pathological continuum of multisystem TDP-43 proteinopathies. *Arch Neurol* 2009;66:180–9.
- Kim EJ, Rabinovici GD, Seeley WW, *et al*. Patterns of MRI atrophy in tau positive and ubiquitin positive frontotemporal lobar degeneration. *J Neurol Neurosurg Psychiatr* 2007;78:1375–8.
- Rohrer JD, Lashley T, Schott JM, *et al*. Clinical and neuroanatomical signatures of tissue pathology in frontotemporal lobar degeneration. *Brain* 2011;134(Pt 9):2565–81.
- McMillan CT, Brun C, Siddiqui S, *et al*. White matter imaging contributes to the multimodal diagnosis of frontotemporal lobar degeneration. *Neurology* 2012;78:1761–8.
- Avants BB, Cook PA, Ungar L, *et al*. Dementia induces correlated reductions in white matter integrity and cortical thickness: a multivariate neuroimaging study with sparse canonical correlation analysis. *NeuroImage* 2010;50:1004–16.
- Forman MS, Farmer J, Johnson JK, *et al*. Frontotemporal dementia: clinicopathological correlations. *Ann Neurol* 2006;59:952–62.
- Otvos L, Feiner L, Lang E, *et al*. Monoclonal antibody PHF-1 recognizes tau protein phosphorylated at serine residues 396 and 404. *J Neurosci Res* 1994;39:669–73.
- Lippa CF, Rosso AL, Stutzbach LD, *et al*. Transactive response DNA-binding protein 43 burden in familial Alzheimer disease and Down syndrome. *Arch Neurol* 2009;66:1483–8.
- Neumann M, Kwong LK, Lee EB, *et al*. Phosphorylation of S409/410 of TDP-43 is a consistent feature in all sporadic and familial forms of TDP-43 proteinopathies. *Acta Neuropathol* 2009;117:137–49.
- Mackenzie IRA, Neumann M, Baborie A, *et al*. A harmonized classification system for FTLT-TDP pathology. *Acta Neuropathol* 2011;122:111–13.
- Mirra SS, Heyman A, McKeel D, *et al*. The Consortium to Establish a Registry for Alzheimer's Disease (CERAD). Part II. Standardization of the neuropathologic assessment of Alzheimer's disease. *Neurology* 1991;41:479–86.
- Brettschneider J, Van Deerlin V, Robinson JL, *et al*. Ubiquitin pathology in ALS and FTLT is determined by the presence of C9orf72 hexanucleotide expansion. *Acta Neuropathol* (in press).
- Yu C-E, Bird TD, Bekris LM, *et al*. The spectrum of mutations in progranulin: a collaborative study screening 545 cases of neurodegeneration. *Arch Neurol* 2010;67:161–70.
- Avants BB, Epstein CL, Grossman M, *et al*. Symmetric diffeomorphic image registration with cross-correlation: evaluating automated labeling of elderly and neurodegenerative brain. *Med Image Anal* 2008;12:26–41.
- Das SR, Avants BB, Grossman M, *et al*. Registration based cortical thickness measurement. *NeuroImage* 2009;45:867–79.
- Cook P, Bai Y, Nedjati-Gilani S. Camino: open-source diffusion-MRI reconstruction and processing. *Int Soc Magn Reson Imaging Med* 2006;27:59.
- Avants B, Dhillon P, Kandel BM, *et al*. Eigenanatomy improves detection power for longitudinal cortical change. Medical image computing and computer-assisted intervention: MICCAI, 2012:206–13.
- Oishi K, Zilles K, Amunts K, *et al*. Human brain white matter atlas: identification and assignment of common anatomical structures in superficial white matter. *NeuroImage* 2008;43:447–57.
- Whitwell JL, Jack CR, Parisi JE, *et al*. Imaging signatures of molecular pathology in behavioral variant frontotemporal dementia. *J Mol Neurosci* 2011;45:372–8.
- McMillan CT, Avants B, Irwin DJ, *et al*. Can MRI screen for cerebrospinal fluid biomarkers in neurodegenerative disease? *Neurology* 2012;80:132–8.
- Grossman M, Powers J, Ash S, *et al*. Disruption of large-scale neural networks in non-fluent/agrammatic variant primary progressive aphasia associated with frontotemporal degeneration pathology. *Brain Lang* 2012; (in press).
- Toledo JB, Brettschneider J, Grossman M, *et al*. CSF biomarkers cutoffs: the importance of coincident neuropathological diseases. *Acta Neuropathol* 2012;24:23–35.
- The National Institute on Aging, and Reagan Institute Working Group on Diagnostic Criteria for the Neuropathological Assessment of Alzheimer's Disease. Consensus recommendations for the postmortem diagnosis of Alzheimer's disease. *Neurobiol Aging* 1997;19:1–2.
- Dickerson BC, Wolk DA, On behalf of the Alzheimer's Disease Neuroimaging Initiative. MRI cortical thickness biomarker predicts AD-like CSF and cognitive decline in normal adults. *Neurology* 2012;78:84–90.
- Hu WT, McMillan C, Libon D, *et al*. Multimodal predictors for Alzheimer disease in nonfluent primary progressive aphasia. *Neurology* 2010;75:595–602.
- Pereira JMS, Williams GB, Acosta-Cabrero J, *et al*. Atrophy patterns in histologic vs clinical groupings of frontotemporal lobar degeneration. *Neurology* 2009;72:1653–60.
- Whitwell JL, Weigand SD, Boeve BF, *et al*. Neuroimaging signatures of frontotemporal dementia genetics: C9orf72, tau, progranulin and sporadics. *Brain* 2012;135(Pt 3):794–806.
- Rohrer JD, Warren JD. Phenotypic signatures of genetic frontotemporal dementia. *Curr Opin Neurol* 2011;24:542–9.
- Irwin DJ, McMillan CT, Brettschneider J, *et al*. Cognitive decline and reduced survival in C9orf72 expansion Frontotemporal degeneration and Amyotrophic lateral sclerosis. *J Neurol Neurosurg Psychiatr* 2013;84:163–9.
- Rohrer JD, Ridgway GR, Modat M, *et al*. Distinct profiles of brain atrophy in frontotemporal lobar degeneration caused by progranulin and tau mutations. *NeuroImage* 2010;53:1070–6.
- Whitwell JL, Jack CR, Parisi JE, *et al*. Does TDP-43 type confer a distinct pattern of atrophy in frontotemporal lobar degeneration? *Neurology* 2010;75:2212–20.



White matter imaging helps dissociate tau from TDP-43 in frontotemporal lobar degeneration

Corey T McMillan, David J Irwin, Brian B Avants, et al.

J Neurol Neurosurg Psychiatry published online March 9, 2013
doi: 10.1136/jnp-2012-304418

Updated information and services can be found at:
<http://jnp.bmj.com/content/early/2013/03/08/jnp-2012-304418.full.html>

These include:

Data Supplement

"Supplementary Data"

<http://jnp.bmj.com/content/suppl/2013/03/08/jnp-2012-304418.DC1.html>

References

This article cites 35 articles, 4 of which can be accessed free at:

<http://jnp.bmj.com/content/early/2013/03/08/jnp-2012-304418.full.html#ref-list-1>

P<P

Published online March 9, 2013 in advance of the print journal.

Email alerting service

Receive free email alerts when new articles cite this article. Sign up in the box at the top right corner of the online article.

Advance online articles have been peer reviewed, accepted for publication, edited and typeset, but have not yet appeared in the paper journal. Advance online articles are citable and establish publication priority; they are indexed by PubMed from initial publication. Citations to Advance online articles must include the digital object identifier (DOIs) and date of initial publication.

To request permissions go to:

<http://group.bmj.com/group/rights-licensing/permissions>

To order reprints go to:

<http://journals.bmj.com/cgi/reprintform>

To subscribe to BMJ go to:

<http://group.bmj.com/subscribe/>

Topic Collections

Articles on similar topics can be found in the following collections

[Dementia](#) (784 articles)
[Memory disorders \(psychiatry\)](#) (1059 articles)
[Neuropathology](#) (150 articles)
[Radiology](#) (1419 articles)
[Radiology \(diagnostics\)](#) (1064 articles)

Notes

Advance online articles have been peer reviewed, accepted for publication, edited and typeset, but have not yet appeared in the paper journal. Advance online articles are citable and establish publication priority; they are indexed by PubMed from initial publication. Citations to Advance online articles must include the digital object identifier (DOIs) and date of initial publication.

To request permissions go to:

<http://group.bmj.com/group/rights-licensing/permissions>

To order reprints go to:

<http://journals.bmj.com/cgi/reprintform>

To subscribe to BMJ go to:

<http://group.bmj.com/subscribe/>